THE INFLUENCE OF FIBRE ANGLE AND RESIN PROPERTIES ON CONSOLIDATION OF CURVED LAMINATES

K. Johnson[1], S. Erland[2] and R. Butler[3]

Department of Mechanical Engineering, University of Bath, Claverton Down, Bath, BA2 7AY, United Kingdom
Email: [1]K.Johnson@bath.ac.uk, [2]S.Erland@bath.ac.uk, [3]R.Butler@bath.ac.uk

Keywords: Consolidation, Fibre angle, Curvature laminates

Abstract

Formability presents a significant contributor to the quality of produced aerospace components. The process of forming is however heavily influenced by the preceding mechanism of laminate consolidation. Understanding the consolidation behaviour of non-flat components gives insight into the coupled effect of temperature and pressure on part quality. The paper presents a theoretical model based on a power law to predict consolidation strains at either end of a curvature laminate for different ranges of temperature and pressure. In addition, investigations outline consolidation behaviour differences of laminates comprising standard and non-standard fibre angles. The model is validated using an experimental tool where laminates are consolidated into a circular female tool, implementing debulking parameters outlined by the theoretical model. All laminate samples produced similar cured thickness, although non-standard fibre angled laminates initially showed reduced consolidation. Contrary to a predicted reduction as a result of restricted inter-ply shear, laminate consolidation improved with increased application of pressure.

1. Introduction

The aerospace industry has a continuously high demand for composite materials to be used in structural applications. The reduction in cost of manufacturing structural composite parts has been established as the key area which requires advancement, in order to make more composite application feasible. Formability presents a vital aspect within the process of manufacturing composite components. This is particularly essential for the widely implemented automated manufacturing techniques, which improve rate of production. The associated risk however, is the generation of defects during the forming process. Prior to a part reaching its final cured part thickness, it has to undergo a debulking stage where both temperature and pressure act in conjunction causing the laminate to consolidate. The majority of composite structures in the aerospace industry feature either some sort of singly or even doubly curved geometry. Therefore, forming parameters such as pressure, which in a plate-like component are very predictable by leading to increased consolidation when subjected to increased pressure, now becomes much more complex. As established by Erland et al. [2], introducing curvature in a geometry results in a need to balance pressure during forming, as it both drives consolidation while restricting inter-ply slip. Two separate aims are investigated in this paper; experimentally validating a model specifically created for a demonstrator part with a curved geometry, and accessing the impact of different quasi-isotropic layups on the consolidation behaviour of the demonstrator.

Excerpt from ISBN 978-3-00-053387-7

2. Theoretical model

In order to understand the coupled effect of pressure, we must consider a scenario in which the pressure applied during debulk or forming invokes some measureable shear strain in the part. A simple way of approaching this is to consider an energy minimisation approach towards deriving the consolidation strain achieved across a curved laminate to which a pressure is applied. This model draws from work done by Dodwell et al. [1], in which a uniform consolidation pressure, σ_n, is applied to the outer layer of a laminate, causing a consolidation strain, η, such that

$$\sigma_n = C\eta(\theta)^2 \tag{1}$$

where C is the consolidation constant derived from fitting experimental data and $\eta(\theta)$ is the actual consolidation strain at angle θ around a curved part. In such a part, formability is influenced by resistance to the shear strain $\gamma(\theta)$ the part must undergo to form, which from [2] can be calculated as:

$$\gamma(\theta) = \ln(1 + \eta_{max}\theta) \tag{2}$$

in which η_{max} is the maximum possible consolidation strain, assumed in this case to be 12% [1,3]. Considering the sample presented in Fig 1., which has a tool angle $\theta = 180^o$, we can see that the shear strain required for the part to form grows from 0 at the clamped edge to a maximum of 0.32 at the free edge by using eqn. 2. The shear strain required for the laminate to consolidate, and by extension the resistance to forming therefore grows around the part, resulting in a potential mismatch in consolidation strain at either end of the part.

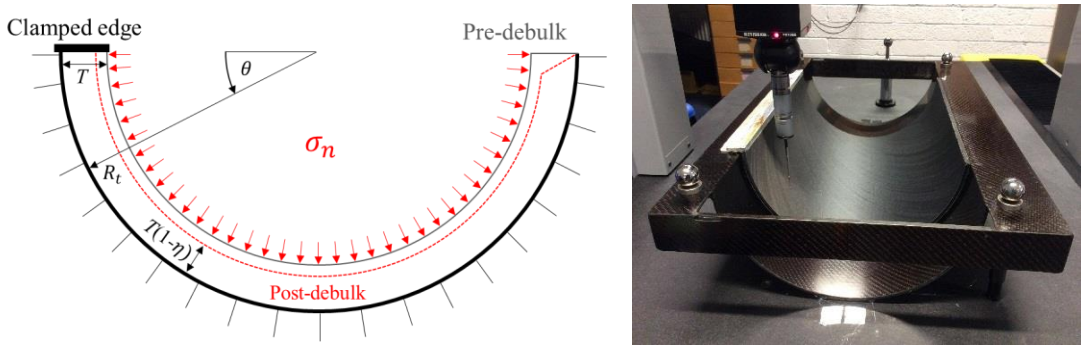

Figure 1: Theoretical and experimental laminate demonstrator in which shear strain is maximised by clamping the left hand edge of the circular part.

Assuming that shear strain increases linearly from 0 at the clamped edge to a maximum value at the free edge, the average consolidation strain across the component is given by:

$$\eta(\theta) = \eta_1 - \eta_2 \frac{\theta}{\pi} \tag{3}$$

where θ is the tool angle. Therefore, as η_2 approaches 0, $\eta(\theta)$ approaches η_1, the maximum consolidation strain. To find η_1 and η_2 we can consider an energy minimisation approach, such that the total energy in the system:

$$V = U_c + U_s - w_\sigma \tag{4}$$

where U_c is the energy in consolidation, such that:

Excerpt from ISBN 978-3-00-053387-7

$$U_C = \int_0^{\theta} \frac{C}{3}\left(\eta(\theta)\right)^3 T R_t \, d\theta \tag{5}$$

where T is laminate thickness and R_t is the tool radius, and U_s is the energy in shear, such that:

$$U_s = \int_0^{\theta} T\tau_C \gamma(\theta)(R_t - T)\, d\theta \tag{6}$$

where τ_C is the critical shear stress from characterisation tests and $\gamma(\theta)$ is the shear strain, such that:

$$\gamma(\theta) = \eta(\theta)\theta \tag{7}$$

and w_σ is the energy in the bag, such that:

$$w_\sigma = \int_0^{\theta} \sigma_n \eta(\theta) T(R_t - T)\, d\theta \tag{8}$$

Substituting eqn. (3) into (5), (6), (7) and (8), and integrating through gives the energy in consolidation as:

$$U_C = \frac{CTR_t}{3}\left(\eta_1^3\theta - \frac{3\eta_1^2\eta_2\theta^2}{2\pi} + \frac{\eta_1\eta_2^2\theta^3}{\pi^2} - \frac{\eta_2^3\theta^4}{4\pi^3}\right) \tag{9}$$

the energy in shear as:

$$U_s = T\tau_c(R_t - T)\left(\frac{\eta_1\theta^2}{2} - \frac{\eta_2\theta^3}{3\pi}\right) \tag{10}$$

and the work done by the bag as:

$$w_\sigma = \sigma_n T(R_t - T)\left(\eta_1\theta - \frac{\eta_2\theta^2}{2\pi}\right) \tag{11}$$

Applying equilibrium, we differentiate V with respect to η_1 and η_2 such that:

$$\frac{\partial V}{\partial \eta_1} = \frac{\partial V}{\partial \eta_2} = 0 \tag{12}$$

This gives us two simultaneous quadratics in η_1 and η_2, which can be solved using Maple [5].

A key limitation with this model is the simplicity of the consolidation law used. The stiffening response modelled in [1] is elastic, and is experimentally derived in a series of relaxation tests from which the resting load value is taken to measure stiffness. This means that the initial temperature and rate-dependent viscous behaviour, exhibited by the resin as it is loaded, is not taken into account. Another limitation is the simplification of the shear energy, which follows a two stage response, with an initial stiffness transitioning to a reduced stiffness after yield. For the purposes of this model we simply use the yield value, τ_c, as an approximation. This results in an over-prediction of the resistance to movement in regions of small shear strain, i.e. pre-yield, and an under-prediction of the resistance in areas of high shear strain, i.e. post yield.

Excerpt from ISBN 978-3-00-053387-7

The values of τ_c used for the model were taken from the 0-0° tests conducted in [4]. In this paper it is noted that τ_c is unaffected by changing interface angle, therefore making the value of τ_c chosen applicable to laminates of varying angled plies. The main influence from angle plies will occur in the post yield region, which is ignored in our simplified model.

Parameters of temperature and pressure were selected using the presented model in order to provide the most significant variation in consolidation strain along the laminate radius. As shown in Table 1, temperatures of 40°C and 80°C, and pressures ranging from 0.05MPa to 0.2MPa were chosen. Although 80°C presented the optimal forming temperature [4], carrying out a debulk procedure at a lower temperature allowed for higher resistance to ply movement, increasing the likeliness of differential consolidation strain around the radius. Consolidation constant *C* values were calculated using the curve fitting app in Matlab, by plotting stress σ_n against consolidation strain η and fitting it to the power law in eqn. 1. The η values for 40°C at the three pressures were taken from the experimental clamped end values from the tests, where shear strain had no influence on consolidation. As there was only one experimental value at 80°C, at 0.2MPa, the values for 0.05 and 0.1MPa were approximated observing the trend set by the 40°C results in order to provide sufficient data to fit to the consolidation law. The tool dimensions used for the model were radius R_t = 150mm and initial laminate thickness T = 5.3mm

Table 1: Modelling parameters used in Section 2 to derive values of $\boldsymbol{\eta_1}$ and $\boldsymbol{\eta_2}$. Values of critical shear stress, $\boldsymbol{\tau_c}$, are calculated using the Mohr-Coulomb model and parameters from [2]. Values of consolidation coefficient C are calculated from a fitted power law, as described in section 2.

Temperature (°C)	σ_n (MPa)	C (MPa)	τ_c (MPa)
40	0.05	57.7	0.00515
	0.1		0.00533
	0.2		0.00571
80	0.2	14.7	0.00413

3. Experimental methodology

The tool design was based around creating a sufficiently long 180° corner that would satisfy the requirements for cured laminate stiffness while incorporating specific design features. CFRP tool material was used due to its low CTE and high rigidity at elevated curing temperatures. The female CFRP tool was moulded from a male aluminium pattern. The dimensions were governed by size limitations of the oven and CMM at the University of Bath, which were used for debulking and laminate scanning procedures. The 180° corner comprises a 150mm radius and 600mm length. Total length and width of the structure was 700mm by 425mm, resulting from added horizontal and vertical flanges. The flanges act as reference planes for creating a coordinate axis system during the CMM set-up, as well as housing four calibration spheres (Fig. 1) while also providing the tool with sufficient stiffness.

Investigated samples included three comparable laminates. One standard quasi-isotropic (QI) laminate and two laminates containing non-standard angles were tested, in which samples were made of AS4/8552 prepreg material and 24 ply stacks. Both the QI and the non-standard laminates have identical in-plane stiffness. The stacking sequences of the investigated laminates are shown below in Table 2. The stacking sequences for 60/0 and 30/90 were determined by minimising bend-twist coupling.

Table 2: Laminate stacking sequences. Note that 90° fibres are circumferential.

Sample ID	Layup
QI	$[(45/\text{-}45/0/90)_3]s$
60/0	$[60/\text{-}60_2/60/\text{-}60/60/0_2/60/\text{-}60/0_2]s$
30/90	$[30/\text{-}30_2/30/\text{-}30/30/90_2/30/\text{-}30/90_2]s$

Excerpt from ISBN 978-3-00-053387-7

Plies were cut with the aid of a template, allowing precision and repeatability concerning overall ply dimensions and angles. A 2mm thick layer of quick curing resin was applied to the left hand laminate edge, acting as a clamping mechanism by bonding the ply ends together. A 4mm thick aluminium plate placed on top of the resin edge during its cure prevented the bag pressure during later debulking steps from distorting the resin edge. Vacuum bagging was performed using non-perforated release film in conjunction with high density breather fabric, to allow optimal removal of air and provide even pressure across the laminate. Debulking cycles at and below atmospheric pressure were carried out in an oven using a needle valve to regulate the given pressure from the vacuum pump. An autoclave was used for debulking that required pressures higher than atmospheric pressure. After each stage of debulk the tool, together with the sample, were securely fixed on the CMM table as shown in Fig. 1. The CMM probe was calibrated prior to each laminate scan using the calibration spheres, in addition to the horizontal and vertical flanges. The probe, with a 2.5mm diameter ruby attached scanned 10 evenly spaced arcs along the laminate length, covering a range of 350mm while neglecting 25mm either side of the 400mm long sample laminate. Within each arc data points were gathered every 1mm along the circumferential axis. The CAD surface generated from the initial tool scan acted as reference for the laminate sample scans, allowing for accurate thickness measurements within tolerances of 4microns. The final cured part thickness was measured by cutting up the samples into 5 semi-circular strips and taking thickness readings every 15° using a micrometer.

4. Experimental and theoretical results

Experimental and predicted values of consolidation strain are shown in Table 1. Consolidation strain at the clamped edge is considered to be the maximum consolidation strain η_1, whilst strain at the free edge is shown as $\eta(180°)$.

Table 3: Predicted and experimental values of consolidation strain

Temperature	**Pressure**	**Predicted**		**Experimental**					
				QI		**60/0**		**30/90**	
(°C)	(MPa)	η_1	$\eta(180°)$	η_1	$\eta(180°)$	η_1	$\eta(180°)$	η_1	$\eta(180°)$
40	0.05	0.029	0.024	0.029	0.037	0.029	0.026	0.031	0.008
	0.1	0.041	0.037	0.036	0.041	0.040	0.035	0.038	0.024
	0.2	0.058	0.055	0.044	0.055	0.053	0.048	0.052	0.033
80	0.2	0.115	0.112	0.108	0.082	0.106	0.089	0.098	0.093
cured	0.7	-	-	0.109	0.100	0.123	0.117	0.119	0.116

Experimental results taken from CMM measurement displaying thickness variation around the radius of the tool are outlined in Figure 2 for the standard QI and 60/0 laminates. Results show fairly small consolidation strains at 40ºC, increasing with applied pressure. Greater levels of consolidation strain are achieved at 80ºC, bringing the part close to final cured part thickness (CPT).

Excerpt from ISBN 978-3-00-053387-7

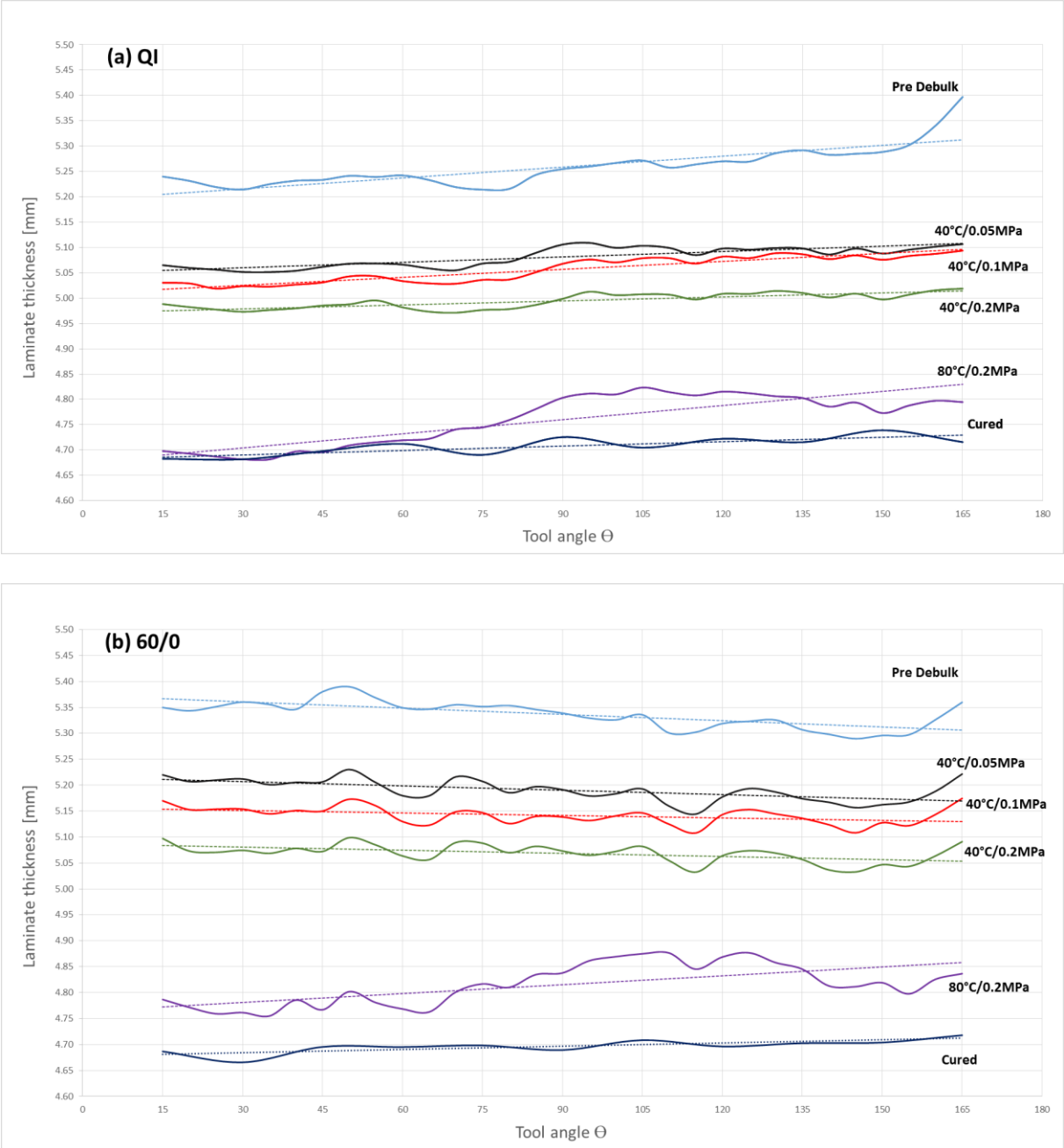

Figure 2 Thickness variation around laminate radius in Fig. 1 at different temperatures and bag pressures $\boldsymbol{\sigma_n}$ for (a) QI and (b) 60/0 laminates

5. Discussion

5.1 Thickness variation traces

The experimental values of η_1 and $\eta(180°)$ from the 40°C debulks were generated by referring to the actual laminate thickness after layup, with its slight thickness variation between both laminate ends arising from a non-perfect hand layup procedure. Measurement data for the initial 15° at the clamped and free laminate edges were removed as a result of edge effects influencing the trendlines and average thickness results. At the clamped edge this occurred as a result of the clamping mechanism itself preventing ply thinning during consolidation, while the lack of edge bars at the free edge allow pressure to act on the ends of the plies, pushing them into the laminate and resulting in local thickening. The

Excerpt from ISBN 978-3-00-053387-7

80°C consolidation strains were calculated assuming a constant pre-debulk laminate thickness around the radius using the average thickness value from the pre-debulk trace, in order to allow for a meaningful analysis of the results. The reasoning behind this is that the nature of the resin in the composite is very different at 40 and 80ºC. At low temperatures, the resin is very viscous, and behaves almost as a plastic solid. At higher temperatures the viscosity drops dramatically, and it becomes a flowing liquid. This is discussed in more detail in the following section.

The thickness results agree with the temperature findings in [2], showing 80ºC to allow for significantly higher degrees of consolidation strain than 40ºC, as a result of the resin have a much lower viscosity at this temperature. In fact, the laminate comes very close to final cure part thickness, which is achieved with a much higher pressure of 0.7MPa at a temperature of 180ºC. As discussed in the next section, this poses problems with the consolidation model used.

5.2 Comparison of predicted vs. experimental consolidation strains

By relating the experimental values of consolidation strain (Table 3) at either edge of the part to those calculated using the model derived in section 2, we can assess both the impact of stacking sequence on the formability of the component, and the accuracy of the energy minimisation model. Starting first with the QI stack, we see that the initial value of η_1 at 40ºC is identical to that predicted by the model, however subsequent predictions overestimate the value of consolidation strain significantly. This is due to the power law used to derive the consolidation coefficient being unsuitable, particularly at higher pressures. To improve its accuracy, the exponent itself in eqn. (1) could be fitted, such that $\sigma_n = C\eta^b$. A more realistic law would use a hyperbolic function, e.g. $\sigma_n = \alpha(\eta_{max} - \eta)^{-1}$, which will be investigated in future work. Whilst the values of consolidation strain at the free edge of the part, $\eta(180°)$, agree in absolute terms, the model predicts that consolidation will reduce around the part. This is not observed for the QI laminate at 40°C, but is apparent for all other cases. The values of $\eta(180°)$ for the QI laminate appear to suggest a negative value of η_2, suggesting that resistance to shear actually aids consolidation. It is thought that these values are the result of some localised voiding during the lay-up, resulting in artificially easier debulking in that region, and a larger apparent consolidation strain. This seems to be apparent in the thickness trace in Fig 2 (a), where there is a sharp increase in pre-debulk thickness as the angle approaches 180º, affecting the gradient of the trendline.

The values of η_1 for the 60/0 laminate agree well with the predictions of the model, suggesting that stacking sequence has influence on ease of consolidation even for a flat plate. The difference in behaviour when compared to the QI laminate highlights the potential requirement for a stacking sequence-specific consolidation coefficient. The values of $\eta(180°)$ fit well with the prediction of the model. This suggests that this stacking sequence increases the resistance to shear strain, compared with the QI laminate. Considering the work in [4, 6] this could be due to the increased number of blocked plies in the 60/0 case, which inhibit through-thickness shear strain, and the lack of any orthotropic interfaces, which promote shear. The benefits of this laminate may become apparent at very high shear strains, i.e. drape forming, which could not be achieved using this test setup. For the 30/90 laminate the η_1 predictions from the model are again accurate. As this laminate resembles the 60/0 case, this is unsurprising and reinforces the apparent influence of stacking sequence on the formability of a flat plate. Values of $\eta(180°)$ show an even greater resistance to shear strain. Again, this is largely due to the regions of blocked 90° plies. From [3] we can see that continuous fibres running around a feature can prevent consolidation if they are unable to accommodate shear strain, further reducing formability.

When comparing the thickness variations along the tool radius for the different experimental laminates, see Fig. 2, it becomes apparent that, at a 40°C debulk temperature, all samples follow a trend set out by the initial pre-debulk thickness distribution. This is even apparent with the QI stack having an initial positive thickness gradient around the tool radius, while the 60/0 laminate is initially negative. The 0.2MPa, 80°C debulk however produces an interesting behaviour where the laminate significantly thickens halfway around the radius towards the free edge. This effect is equally present in all three

Excerpt from ISBN 978-3-00-053387-7

laminate samples and seems to be a side effect of the bag pressure on the free edge. At this temperature and pressure, the QI laminate already reaches final cured part thickness in the first 60° of the tool radius. While having the same thickness distribution around the radius as the QI, the non-standard 60/0 laminate however does not reach cured ply thickness at this stage due to the previously mentioned non-standard stacking sequence characteristics. Despite having different initial average thicknesses and thickness distributions, all samples achieve an identical laminate average thickness of 4.7mm after a full cure at 180°C including a small circumferential increase in thickness. Both non-standard laminates reach a maximum consolidation strain at cure of 12%. This value exactly matches the initial assumption made in section 2 for the consolidation strain used for calculating the maximum possible shear strain. The QI laminate however only shows a maximum consolidation strain of 10.5%, which is a result of the slightly thinner average thickness pre debulk.

6. CONCLUSION

In this paper an energy minimisation model capable of predicting consolidation strain around a curved tool was developed and validated against a rigorous experimental setup. The theoretical model, capable of predicting consolidation strains at various temperatures and pressures, presents a useful tool to simulate overall consolidation strain trends for curved laminates. As the implemented power law tends to over predict consolidation strains, utilising a hyperbolic law instead should result in much more accurate predictions, especially at higher pressures. The experimental investigation on consolidation comparison for a standard QI and two non-standard 60/0 and 30/90 laminates outlined that although the QI laminate demonstrates improved consolidation behaviour at lower temperatures, all samples achieved the same cured thickness. Therefore, despite having blocked plies in the non-standard stacking sequence, the laminates ultimately show equal consolidation performance based on final part quality.

Using both theoretical models and experimental tests, investigations have demonstrated that pressure does not significantly prevent consolidation strain in curved laminates. In order for pressure to have a more significant effect, higher shear strains need to be achieved. Future work should therefore focus on using a demonstrator with double curvature and utilising a forming procedure such as hot drape forming.

Acknowledgements

The authors thank Steve Thomas for technical assistance and Andrew Francis for developing the CMM code. We also thank GKN Aerospace for the supply of AS4/8552 material. Richard Butler holds a Royal Academy of Engineering/GKN Aerospace Research Chair in Composite Analysis.

References

[1] T.J. Dodwell, R. Butler and G.W. Hunt, Out-of-plane ply wrinkling defect during consolidation over and external radius, Composites Science and Technology, 105, 2014, pp. 151-159.
[2] S. Erland, T.J. Dodwell, R. Butler, Characterisation of inter-ply shear in uncured carbon fibre prepreg, Composites Part A, 77, 2015, pp. 210-228.
[3] T.A. Fletcher, R. Butler and T.J. Dodwell, Anti-symmetric laminates for improved consolidation and reduced warp of tapered C-sections, Advanced Manufacturing: Polymer and Composites Science, 1(2), 2015, pp. 105-111.
[4] S. Erland, T.J. Dodwell and R. Butler, The influence of fibre angle and resin properties on uncured interplay shear, ECCM17 - 17th European Conference on Composite Materials, Munich, Germany, 26-30th June 2016
[5] Dodwell TJ, Erland S, Butler R. A Cosserat continuum model for uncured composite laminates with applications to ply wrinkle formation, ICCM20 – 20th International Conference on Composite Materials, Copenhagen, 19th-24th July, 2015
[6] P. Hallander, M. Akermo, C. Mattei, M. Petersson and T. Nyman, An experimental study of mechanisms behind wrinkle development during forming of composite laminates, Composites Part A, 50, 2013, pp. 54-64.

Excerpt from ISBN 978-3-00-053387-7